ACS APPLIED MATERIALS & INTERFACES

Research Article

www.acsami.org

Photocatalytic Properties of Layered Metal Oxides Substituted with Silver by a Molten $AgNO_3$ Treatment

Hirotaka Horie,[†] Akihide Iwase,[†,‡] and Akihiko Kudo*[,†,‡]

[†]Department of Applied Chemistry, Faculty of Science, Tokyo University of Science, 1-3 Kagurazaka, Shinjuku-ku, Tokyo 162-8601, Japan

[‡]Photocatalysis international Research Center, Research Institute for Science and Technology, Tokyo University of Science, 2641 Yamazaki, Noda-shi, Chiba 278-8510, Japan

Supporting Information

ABSTRACT: $K_4Nb_6O_{17}$ (BG: 3.67 eV) and $Na_2W_4O_{13}$ (BG: 3.12 eV) layered oxide photocatalysts with wide band gaps were treated with a molten $AgNO_3$ to substitute K^+ and Na^+ with Ag^+, resulting in red-shifts of absorption edges in diffuse reflectance spectra. A part of Na^+ ions in the interlayer of $Na_2W_4O_{13}$ was substituted with Ag^+ ions by the molten $AgNO_3$ treatment with keeping the layered structure. Both Ag(I)-substituted $K_4Nb_6O_{17}$ and $Na_2W_4O_{13}$ showed photocatalytic activities for O_2 evolution from aqueous solutions containing a sacrificial reagent utilizing the absorption bands newly formed by the Ag(I)-substitution. Notably, the Ag(I)-substituted $Na_2W_4O_{13}$ produced O_2 under visible light irradiation. When ball-milled $Na_2W_4O_{13}$ was treated with a molten $AgNO_3$, the Ag(I)-substitution rate increased. The Ag(I)-substituted $Na_2W_4O_{13}$ with ball-milling showed higher photocatalytic activity for O_2 evolution than that without ball-milling. Z-schematic water splitting proceeded under visible light irradiation by combining the Ag(I)-substituted $Na_2W_4O_{13}$ of an O_2-evolving photocatalyst with Ru-loaded $SrTiO_3$ doped with Rh of a H_2-evolving photocatalyst.

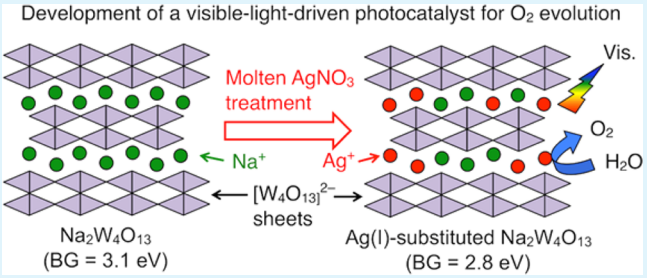

KEYWORDS: *photocatalysis, molten salt, band engineering, Z-scheme, water splitting, visible light*

1. INTRODUCTION

Photocatalytic water splitting using metal oxides is an attractive reaction to address energy and environmental issues. Many metal oxide photocatalysts for water splitting under UV light irradiation have been reported so far.[1,2] Among them, metal oxides with layered structure are a promising material group for efficient water splitting. For example, $K_4Nb_6O_{17}$ with unique interlayers in which reduction sites are separated from oxidation sites splits water without a cocatalyst.[3] Moreover, $Na_2W_4O_{13}$ with 3.1 eV of a band gap shows activity for sacrificial H_2 and O_2 evolution under UV irradiation.[4] However, in order to utilize abundant solar energy, visible light response is indispensable.

GaN−ZnO solid solution,[5] $ZnGeN_2$−ZnO solid solution,[6] Rh and Sb-codoped $SrTiO_3$,[7] TaON,[8] and $LaMg_xTa_{1-x}O_{1+3x}N_{2-3x}$[9] have been reported as a single particulate photocatalyst for water splitting under visible light irradiation. However, water splitting with one-step photoexcitation under visible light irradiation is still challenging because of limited materials and low efficiencies. In contrast, many photocatalysts for sacrificial H_2 and O_2 evolution under visible light irradiation have been reported, e.g., WO_3,[10] $BiVO_4$,[11] TiO_2/Cr,Sb,[12] $AgNbO_3$,[13] $SrTiO_3$/Cr,Ta,[14] $SrTiO_3$/Rh,[15] $SnNb_2O_6$,[16] $Sm_2Ti_2S_2O_5$,[17] and Ta_3N_5.[18] These photocatalysts can be used for Z-schematic water splitting under visible light irradiation by employing a suitable electron mediator.[19,25] Thus, development of photocatalysts for sacrificial H_2 and O_2 evolution under visible light irradiation is still meaningful.

Forming a new valence band is a useful strategy for sensitizing a wide band gap photocatalyst to visible light. Orbitals of Ag 4d in Ag^+,[13] Bi 6s in Bi^{3+},[11] Cu 3d in Cu^+,[25−29] Sn 5s in Sn^{2+},[16] and Pb 6s in Pb^{2+}[30,31] form new valence bands at higher energy levels than those of O 2p orbitals. For example, Sn(II)-substituted $K_4Nb_6O_{17}$ and $KTiNbO_5$ with layered structure respond to visible light.[32] Visible-light responsive $AgLi_{1/3}M_{2/3}O_2$ with delafossite-type structure can be synthesized by treating Li_2MO_4 (M= Ti and Sn) layered oxide with a molten $AgNO_3$.[33] Thus, the substitution of metal ions in the interlayer to form new and shallow valence bands is an effective strategy for layered metal oxides to develop visible-light driven photocatalysts. Ag(I)-substituted materials of $AgLaNb_2O_7$[34] and $Ag_2La_2Ti_3O_{10}$[35] were also prepared via a molten $AgNO_3$ treatment of $RbLaNb_2O_7$ and $A_2La_2Ti_3O_{10}$ (A = Na, K), respectively, although they are not photocatalysts.

In the present study, Ag(I)-substituted $K_4Nb_6O_{17}$ and $Na_2W_4O_{13}$ were synthesized by treating $K_4Nb_6O_{17}$ and $Na_2W_4O_{13}$ with a molten $AgNO_3$, and their photocatalytic

Received: February 17, 2015
Accepted: June 23, 2015
Published: June 23, 2015

DOI: 10.1021/acsami.5b01555
ACS Appl. Mater. Interfaces 2015, 7, 14638−14643

properties were investigated. Moreover, the $Na_2W_4O_{13}$ was pulverized by ball milling to increase the Ag(I)-substitution rate. Z-Schematic water splitting under visible light irradiation was demonstrated by employing the Ag(I)-substituted $Na_2W_4O_{13}$ as an O_2-evolving photocatalyst.

2. EXPERIMENTAL SECTION

2.1. Preparation of Photocatalysts. Layered $K_4Nb_6O_{17}$[3] and $Na_2W_4O_{13}$[4] with wide band gaps were prepared from K_2CO_3 (Kanto Chemical; 99.5%), Nb_2O_5 (Kojundo Chemical; 99.99%), $Na_2WO_4{\cdot}2H_2O$ (Kanto; 99%), and WO_3 (Nacalai Tesque; 99.5%) by a solid-state reaction, as previously reported. Staring materials were mixed in an alumina mortar in a stoichiometric amount, and the mixtures were calcined in air using a platinum crucible at 1723 K for 15 min for $K_4Nb_6O_{17}$ and 1023 K for 20 h for $Na_2W_4O_{13}$. $Na_2W_4O_{13}$ was pulverized using a planetary ball mill (Fritsch Japan; Pulverisette), if necessary. The ball milling for the powder (1 g) was operated using agate balls (5 g, Φ3.0 mm) and pure water (7 mL) at 400 rpm for 1 h.

Ag(I)-substituted $K_4Nb_6O_{17}$ and $Na_2W_4O_{13}$ were synthesized by molten $AgNO_3$ treatment. The mixtures of $AgNO_3$ (Tanaka Kikinzoku; 99.8%) and either $K_4Nb_6O_{17}$ or $Na_2W_4O_{13}$ in a 1:1 to 10:1 atomic ratio of Ag/alkali were heated at 523−773 K for 3−10 h in a Pyrex glass tube. The obtained Ag(I)-substituted $K_4Nb_6O_{17}$ was washed with water and nitric acid to remove $AgNO_3$ and metallic Ag, respectively. The Ag(I)-substituted $Na_2W_4O_{13}$ was washed with water.

Rh(1 atm%)-doped $SrTiO_3$ of an H_2-evolving photocatalyst in a Z-scheme system was prepared by a conventional solid-state reaction, as previously reported.[15] The starting materials of $SrCO_3$ (Kanto; 99.9%), TiO_2 (Soekawa; 99.9%), and Rh_2O_3 (Wako pure chemical; 99%) were mixed in an atomic ratio of Sr/Ti/Rh = 1.07:1:0.01 in an alumina mortar. The mixture was calcined in an alumina crucible at 1073 K for 1 h and then 1273 K for 10 h.

2.2. Characterization. The crystal phase of the prepared powder was determined using an X-ray diffractometer (Rigaku; MiniFlex). Morphology and particle size of the powder were observed using a scanning electron microscope (Jeol; JSM-6700F). Diffuse reflectance spectra were obtained using a UV−vis−NIR spectrometer (Jasco; UbestV-570) and were converted to absorbance by the Kubelka−Munk method. The Ag(I)-substitution rates in $Na_2W_4O_{13}$ and $K_4Nb_6O_{17}$ were determined using an X-ray fluorescence spectrometer (PANalytical; Epsilon 5) with employing $Na_2WO_4{\cdot}2H_2O$ and Ag_2WO_4 as references of the atomic ratios of Na/W and Ag/W, respectively. The atomic ratios of Ag(I) at the surface of Ag(I)-substituted $Na_2W_4O_{13}$ and the valence band spectra were analyzed using an X-ray photoelectron spectrometer (Jeol; JSP-9010MC).

2.3. Photocatalytic Reaction. Photocatalytic reactions of sacrificial O_2 evolution and Z-schematic water splitting were carried out using a gas-closed circulation system with a top irradiation cell with a Pyrex window. A 300 W Xe-arc lamp (PerkinElmer; Cermax PE-300BF) was employed as a light source. The wavelength of irradiated light was controlled by long-pass filters (L38 or L42, $\lambda > 380$ or 420 nm). The photocatalyst powders (0.2−0.3 g) were dispersed in aqueous solutions (120 mL) containing $AgNO_3$ (20 mmol L^{-1}) and $FeCl_3$ (2 mmol L^{-1}, pH2.4) for the sacrificial O_2 evolution. 0.1 g of Ru(0.3 wt %)-loaded $SrTiO_3$ doped with Rh of a H_2-evolving photocatalyst and 0.15−0.2 g of Ag(I)-substituted $Na_2W_4O_{13}$ of an O_2-evolving photocatalyst were dispersed in 120 mL of aqueous H_2SO_4 (pH3.5) and $FeCl_3$ (2 mmol L^{-1}, pH2.4) solutions for Z-schematic water splitting without and with an electrum mediator. The pH of the aqueous $FeCl_3$ solution was adjusted with H_2SO_4. The amounts of evolved H_2 and O_2 were determined by a gas chromatograph (Shimadzu; MS-5A column, TCD, Ar carrier).

3. RESULTS AND DISCUSSION

3.1. Synthesis of Ag(I)-Substituted Layered Oxides and Their Physicochemical Properties. Layered oxides of $K_4Nb_6O_{17}$ and $Na_2W_4O_{13}$ were treated with a molten $AgNO_3$ at 573 K for 3 h to substitute K^+ ions in $K_4Nb_6O_{17}$ and Na^+ ions in $Na_2W_4O_{13}$ with Ag^+ ions. Figures 1 and 2 show XRD patterns and diffuse reflectance spectra of $K_4Nb_6O_{17}$ and $Na_2W_4O_{13}$ with and without a molten $AgNO_3$ treatment, respectively.

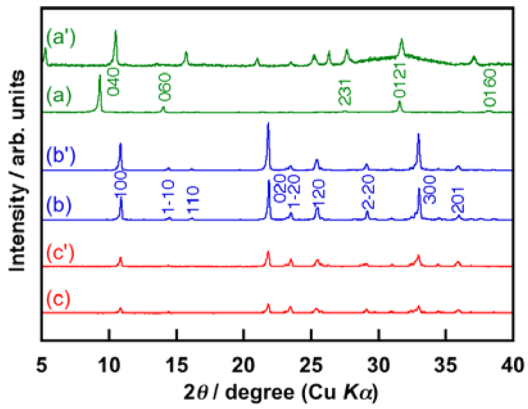

Figure 1. XRD patterns of (a) $K_4Nb_6O_{17}$, (a′) Ag(I)-$K_4Nb_6O_{17}$, (b) $Na_2W_4O_{13}$, (b′) Ag(I)-$Na_2W_4O_{13}$, (c) milled-$Na_2W_4O_{13}$, and (c′) Ag(I)-milled-$Na_2W_4O_{13}$. Ag(I)-$K_4Nb_6O_{17}$ was obtained by a molten $AgNO_3$ treatment at 573 K for 3 h (Ag^+/K^+ = 1.2:1). Ag(I)-$Na_2W_4O_{13}$ and Ag(I)-milled-$Na_2W_4O_{13}$ were obtained by a molten $AgNO_3$ treatment at 523 K for 5 h (Ag^+/Na^+ = 2:1). PDFs 21-1297 and 21-1167 were referred for Miller indices.

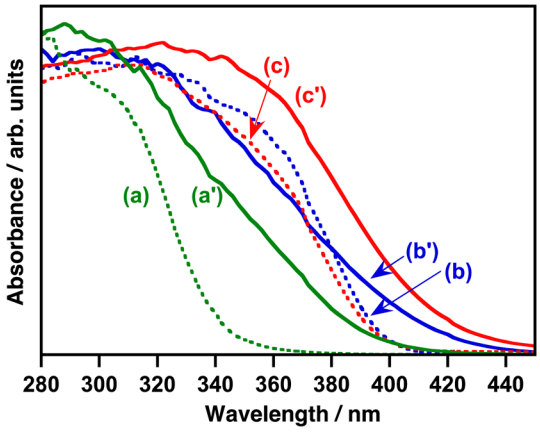

Figure 2. Diffuse reflectance spectra of (a) $K_4Nb_6O_{17}$, (a′) Ag(I)-$K_4Nb_6O_{17}$, (b) $Na_2W_4O_{13}$, (b′) Ag(I)-$Na_2W_4O_{13}$, (c) milled-$Na_2W_4O_{13}$, and (c′) Ag(I)-milled-$Na_2W_4O_{13}$. Ag(I)-$K_4Nb_6O_{17}$ was obtained by a molten $AgNO_3$ treatment at 573 K for 3 h (Ag^+/K^+ = 1.2:1). Ag(I)-$Na_2W_4O_{13}$ and Ag(I)-milled-$Na_2W_4O_{13}$ were obtained by a molten $AgNO_3$ treatment at 523 K for 5 h (Ag^+/Na^+ = 2:1).

The (040) and (060) peaks at 9.3° and 14° due to interlayer of $K_4Nb_6O_{17}$ shifted to higher degree after a molten $AgNO_3$ treatment (Figure 1, parts a and a′). This shift is reasonable, judging from a smaller ionic radius for Ag^+ ion (1.28 Å for 8 coordination) than that for K^+ ion (1.51 Å for 8 coordination).[36] Moreover, SEM observation revealed that Ag(I)-substituted $K_4Nb_6O_{17}$ was plate shaped, which is the same shape as the sample before a molten $AgNO_3$ treatment (Supporting Information, SI, Figure S1). Thus, the treated $K_4Nb_6O_{17}$ still kept a layered structure because of the high ion-exchange capacity of $K_4Nb_6O_{17}$.[37] The XRF measurement revealed that 83% of K^+ ions was substituted with Ag^+ in the treated $K_4Nb_6O_{17}$, as shown in Table 1. Moreover, the absorption edge of $K_4Nb_6O_{17}$ red-shifted by a molten $AgNO_3$

DOI: 10.1021/acsami.5b01555
ACS Appl. Mater. Interfaces 2015, 7, 14638−14643

Table 1. Photocatalytic Activities of Ag(I)-Substituted $K_4Nb_6O_{17}$ and $Na_2W_4O_{13}$ Prepared by a Molten $AgNO_3$ Treatment for O_2 Evolution from Aqueous Solutions Containing Sacrificial Reagents

entry	photocatalyst	Ag(I)- substitution rate[a]	EG (eV)	incident light (nm)	sacrificial reagent	activity[b] (μmol h^{-1})
1	$K_4Nb_6O_{17}$	0	3.67	$\lambda > 380$	Ag^{+c}	0.9
2	$K_4Nb_6O_{17}$	0	3.67	$\lambda > 420$	Ag^{+c}	0.4
3	Ag(I)-$K_4Nb_6O_{17}$	0.83	3.13	$\lambda > 380$	Ag^{+c}	3.9
4	Ag(I)-$K_4Nb_6O_{17}$	0.83	3.13	$\lambda > 420$	Ag^{+c}	0.7
5	$Na_2W_4O_{13}$	0	3.12	$\lambda > 420$	Ag^{+c}	trace
6	$Na_2W_4O_{13}$	0	3.12	$\lambda > 420$	Fe^{3+d}	0
7	Ag(I)-$Na_2W_4O_{13}$	0.31	2.88	$\lambda > 420$	Ag^{+c}	0.9
8	Ag(I)-$Na_2W_4O_{13}$	0.31	2.88	$\lambda > 420$	Fe^{3+d}	4.3
9	Ag(I)-milled-$Na_2W_4O_{13}$	0.40	2.82	$\lambda > 420$	Ag^{+c}	3.8
10	Ag(I)-milled-$Na_2W_4O_{13}$	0.40	2.82	$\lambda > 420$	Fe^{3+d}	11

[a]Atomic rate of $Ag^+/(Ag^+ + K^+ \text{ or } Na^+)$ estimated from XRF. [b]Catalyst: 0.3 g, light source: 300 W Xe-arc lamp with a long-pass filter ($\lambda > 420$ and 380 nm), solution: 120 mL, [c]20 mmol L^{-1} of $AgNO_{3\ aq}$. [d]2 mmol L^{-1} of $FeCl_{3\ aq}$ at pH 2.4.

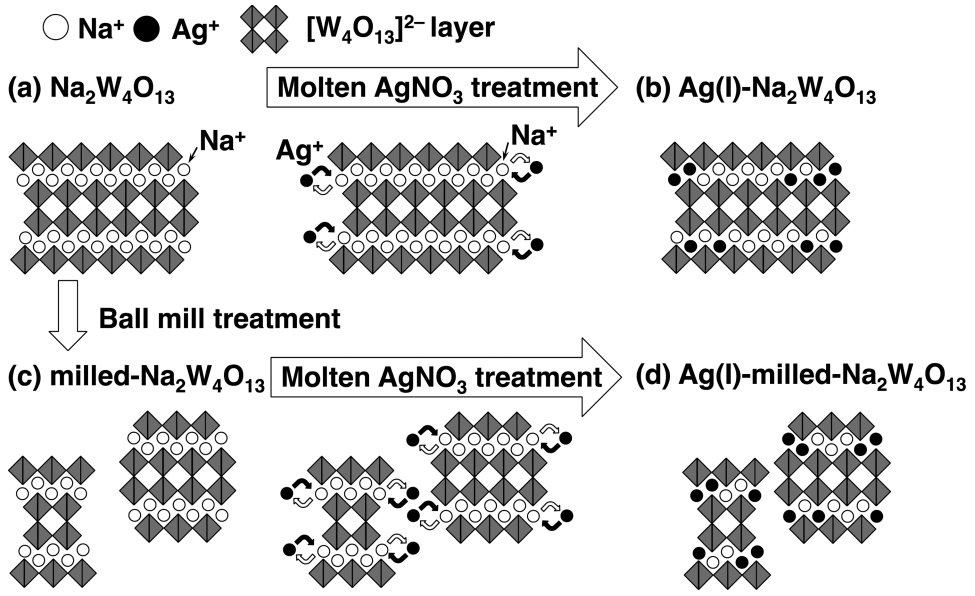

Figure 3. Proposed schematic mechanism of the synthesis of Ag(I)-substituted $Na_2W_4O_{13}$ by a molten $AgNO_3$ treatment. (a) $Na_2W_4O_{13}$, (b) Ag(I)-$Na_2W_4O_{13}$, (c) milled-$Na_2W_4O_{13}$, and (d) Ag(I)-milled-$Na_2W_4O_{13}$.

treatment (Figure 2, parts a and a′). We have previously reported that Ag 4d orbitals form a valence band at higher energy level than O 2p orbitals.[13,33] Therefore, the red-shift was due to the formation of a niobate containing Ag^+ ions. Here, the $K_4Nb_6O_{17}$ with the molten $AgNO_3$ treatment was denoted as Ag(I)-$K_4Nb_6O_{17}$.

The XRD pattern of $Na_2W_4O_{13}$ with a molten $AgNO_3$ treatment was the same as that without a molten $AgNO_3$ treatment (Figure 1, parts b and b′). The shift in the XRD pattern indicated that lattice parameters a and c were shortened and lengthened, respectively (SI Figure S2). The *a* axis normal to interlayer usually became long, when Ag^+ ions (1.28 Å for 8 coordination) were exchanged for Na^+ ions (1.18 Å for 8 coordination) in the interlayer.[36] A possible reason for this contradictory phenomenon would be that the substituted Ag^+ ion occupies different position from Na^+ ion, as observed for $Na_2Ti_6O_{13}$–$Li_2Ti_6O_{13}$ system.[38] XPS and XRF measurements also indicated the existence of Ag^+ ions in the $Na_2W_4O_{13}$ with molten $AgNO_3$ treatment, as shown in Table 1. Moreover, the absorption edge of $Na_2W_4O_{13}$ red-shifted into the visible light region by molten $AgNO_3$ treatment, as shown in Figure 2. To clarify if the red-shift was due to the Ag(I)-substitution, the valence band spectra of $Na_2W_4O_{13}$ with and without a molten $AgNO_3$ treatment were analyzed by XPS (SI Figure S3). The onset of a binding energy for $Na_2W_4O_{13}$ with a molten $AgNO_3$ treatment was smaller than that of nontreated $Na_2W_4O_{13}$, indicating that shallower valence bands were formed by a molten $AgNO_3$ treatment. These characterizations revealed that a part of Na^+ ions in interlayer of $Na_2W_4O_{13}$ were substituted with Ag^+ ions by a molten $AgNO_3$ treatment with keeping the layered structure. Therefore, $Na_2W_4O_{13}$ with a molten $AgNO_3$ treatment was denoted as Ag(I)-$Na_2W_4O_{13}$. Since Ag(I)-$Na_2W_4O_{13}$ possessed a small absorption in visible light region, it is expected to show photocatalytic activity under visible light irradiation.

The poor visible light absorption of Ag(I)-$Na_2W_4O_{13}$ will be due to the low Ag(I)-substitution rate as shown in Table 1. The total Ag(I)-substitution rate in Ag(I)-$Na_2W_4O_{13}$ was determined to be 0.31 by an XRF measurement. The Ag(I)-substitution rate at the surface of Ag(I)-$Na_2W_4O_{13}$ was estimated to be 0.68 by an XPS measurement. Higher Ag(I)-substitution rate at the surface than the total Ag(I)-substitution rate would be due to the large particle of $Na_2W_4O_{13}$, having a size of several micrometers to several tens micrometers. The

DOI: 10.1021/acsami.5b01555
ACS Appl. Mater. Interfaces 2015, 7, 14638−14643

$Na_2W_4O_{13}$ remained as a large particle even after the molten $AgNO_3$ treatment (SI Figure S1, parts c and d). Since the Na^+ ions should be substituted with Ag^+ ions from the edge of the interlayer, as shown in Figure 3, Na^+ ions located inside the interlayer was insufficiently exchanged. We have tried molten $AgNO_3$ treatments with long time of 15 h and high ratio of Ag/Na of 5:1 to increase the Ag(I)-substitution rate and visible light absorption (SI Figure S4). However, XRD patterns and diffuse reflectance spectra of both Ag(I)-$Na_2W_4O_{13}$ samples were almost the same as those of Ag(I)-$Na_2W_4O_{13}$ obtained by a molten $AgNO_3$ treatment at 523 K for 5 h (Ag^+/Na^+ = 2:1). This result indicates that a change in the molten $AgNO_3$ treatment conditions does not increase the Ag(I)-substitution rate at least in our method. Therefore, forming small particles will increase the Ag(I)-substitution rate.

The particle size of $Na_2W_4O_{13}$ decreased to from 1 μmto several μm by ball milling (SI Figure S3e). The XRD pattern and the absorption edge of the $Na_2W_4O_{13}$ with ball milling were the same as those of nontreated $Na_2W_4O_{13}$ as shown in Figures 1 and 2. When the milled $Na_2W_4O_{13}$ was treated by a molten $AgNO_3$ (Ag(I)-milled-$Na_2W_4O_{13}$), 0.95 and 0.40 of the Ag(I)-substitution rate at the surface and the total Ag(I)-substitution rate were achieved, respectively. Both rates were higher than those of Ag(I)-$Na_2W_4O_{13}$ without milling (0.68 and 0.31), as shown in Table 1. Thus, the Ag(I)-substitution rate was successfully increased by forming small particles. The increase in the Ag(I)-substitution rate improved the intensity of the absorption due to the Ag(I)-related excitation, as shown in Figure 2.

3.2. Photocatalytic O_2 Evolution over Ag(I)-Substituted Layered Oxides in the Presence of Sacrificial Reagents. Photocatalytic activities for sacrificial O_2 evolution over Ag(I)-$K_4Nb_6O_{17}$, Ag(I)-$Na_2W_4O_{13}$, and Ag(I)-milled-$Na_2W_4O_{13}$ were evaluated not only under visible light, but also under the light corresponding to the new absorption bands formed by Ag(I)-substitution, as shown in Table 1. Lights with wavelengths longer than 380 nm for Ag(I)-$K_4Nb_6O_{17}$ and 420 nm for Ag(I)-$K_4Nb_6O_{17}$, Ag(I)-$Na_2W_4O_{13}$, and Ag(I)-milled-$Na_2W_4O_{13}$ were employed to avoid the band gap excitation of $K_4Nb_6O_{17}$ and $Na_2W_4O_{13}$, judging from their absorption edges shown in Figure 2.

Nontreated $K_4Nb_6O_{17}$ evolved a small amount of O_2 in the presence of $AgNO_3$ under irradiation of light longer than 380 and 420 nm (Entries 1 and 2) in spite of the fact that it cannot absorb the photons at those wavelength ranges (Figure 2). This is probably because K^+ ions in $K_4Nb_6O_{17}$ were exchanged for Ag^+ ions in an aqueous $AgNO_3$ solution due to the high ion-exchange capacity of $K_4Nb_6O_{17}$.[39] In fact, the absorption edge shifted to a longer wavelength at around 380 nm by just stirring $K_4Nb_6O_{17}$ powder into an aqueous $AgNO_3$ solution (SI Figure S5). The Ag(I)-$K_4Nb_6O_{17}$ showed higher activity under irradiation of light longer than 380 nm than that of nontreated $K_4Nb_6O_{17}$ (Entries 1 and 3). This indicates the priority of Ag(I)-substitution by a molten $AgNO_3$ treatment compared to Ag(I)-exchange by stirring in an aqueous $AgNO_3$ solution in the sensitization of the $K_4Nb_6O_{17}$ photocatalyst to longer wavelength. Characteristic XRD peaks at around 5.3°, 10.5°, and 15.7° due to the interlayer still remained even after photocatalytic O_2 evolution (SI Figure S6A), indicating that the Ag(I)-$K_4Nb_6O_{17}$ worked steadily as a photocatalyst.

$Na_2W_4O_{13}$ showed negligible activities for O_2 evolution from aqueous $AgNO_3$ and $FeCl_3$ solutions under visible light irradiation (Entries 5 and 6). In contrast, Ag(I)-$Na_2W_4O_{13}$ and Ag(I)-milled-$Na_2W_4O_{13}$ produced O_2 under visible light irradiation (Entries 7−10). The activities in an aqueous $FeCl_3$ solution were higher than those in an aqueous $AgNO_3$ solution. Ag(I)-$Na_2W_4O_{13}$ after photocatalytic O_2 evolution from an aqueous $FeCl_3$ solution also possessed a similar XRD pattern to that before the reaction (SI Figure S6B), indicating the stability of Ag(I)-$Na_2W_4O_{13}$. Ag(I)-milled-$Na_2W_4O_{13}$ showed higher activities than Ag(I)-$Na_2W_4O_{13}$ under visible light irradiation. This enhancement was due to the increase in the absorption intensity at the visible light region by the increase in the Ag(I)-substitution rate as well as the decrease in the distance that photogenerated electrons and holes have to migrate by the decrease in the particle size. Thus, the visible-light-responsive Ag(I)-$Na_2W_4O_{13}$ and Ag(I)-milled-$Na_2W_4O_{13}$ were developed by Ag(I)-substitution.

Figure 4 shows the time courses of O_2 evolution over Ag(I)-milled-$Na_2W_4O_{13}$ in the presence and absence of Fe^{3+} ions

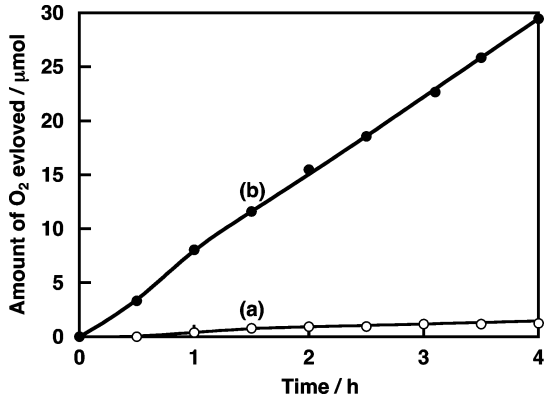

Figure 4. Photocatalytic O_2 evolution over Ag(I)-milled-$Na_2W_4O_{13}$ under visible light irradiation from (a) water and (b) an aqueous $FeCl_3$ solution (2 mmol L^{-1}). Catalyst: 0.3 g, solution; 120 mL, light source: 300 W Xe-arc lamp with a long-pass filter (λ > 420 nm).

under visible light irradiation. Ag(I)-milled-$Na_2W_4O_{13}$ steadily produced O_2 from an aqueous $FeCl_3$ solution without any noticeable degradation. A small amount of O_2 evolved even in the absence of Fe^{3+} ions, indicating that a part of Ag^+ ions in Ag(I)-milled-$Na_2W_4O_{13}$ were reduced by photogenerated electrons. However, the rate of O_2 evolution in the presence of Fe^{3+} ions was much faster than that in the absence of Fe^{3+}. This indicates that most of the Ag^+ ions stably remained in the interlayer and that mainly O_2 evolved, accompanied by consuming Fe^{3+} of an electron acceptor.

Figure 5 shows an action spectrum for O_2 evolution over Ag(I)-milled-$Na_2W_4O_{13}$ from an aqueous $FeCl_3$ solution. Ag(I)-milled-$Na_2W_4O_{13}$ responded to visible light up to 440 nm. The onset of the action spectrum agreed well with the edge of the absorption band formed by Ag(I)-substitution. This agreement indicates that the O_2 evolution proceeded accompanied by the transition from the new valence band consisting of Ag 4d orbitals to the conduction band consisting of W 5d orbitals as observed for some Ag-containing metal oxide photocatalysts.[12]

3.3. Z-Schematic Water Splitting in Visible Light Using Ag(I)-Milled $Na_2W_4O_{13}$ as an O_2-Evolving Photocatalyst. The Ag(I)-milled-$Na_2W_4O_{13}$ of an O_2-evolving photocatalyst was applied to the Z-schematic water splitting with $Fe^{3+/2+}$ of a redox couple and Ru-loaded $SrTiO_3$ doped with Rh (Ru/$SrTiO_3$/Rh) of a H_2-evolving photocatalyst as

DOI: 10.1021/acsami.5b01555
ACS Appl. Mater. Interfaces 2015, 7, 14638−14643

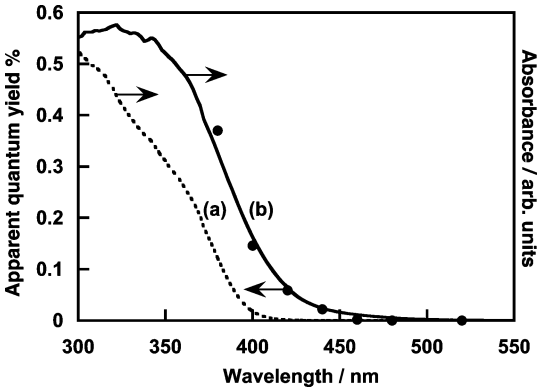

Figure 5. Action spectrum of O_2 evolution over Ag(I)-milled-$Na_2W_4O_{13}$ from an aqueous $FeCl_3$ solution and diffuse reflectance spectra of (a) $Na_2W_4O_{13}$ and (b) Ag(I)-milled-$Na_2W_4O_{13}$.

shown in Figure 6. O_2 evolved dominantly with deviation from the stoichiometric water splitting until 15 h of irradiation time

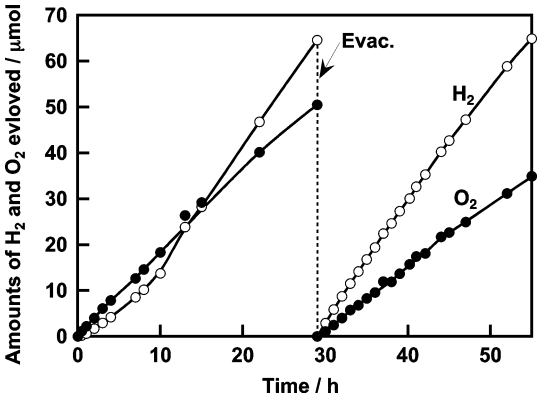

Figure 6. Z-Schematic water splitting into H_2 and O_2 using (Ru/$SrTiO_3$/Rh)-(Ag(I)-milled-$Na_2W_4O_{13}$)-($Fe^{3+/2+}$) under visible light irradiation. Catalyst: 0.1 g of Ru/$SrTiO_3$/Rh, 0.15 g of Ag(I)-milled-$Na_2W_4O_{13}$, solution: 120 mL of 2 mmol L^{-1} of $FeCl_{3aq}$ (pH 2.4), light source: 300 W Xe-arc lamp with a long-pass filter (λ > 420 nm).

because of the use of an aqueous $FeCl_3$ solution as a reactant solution (first run in Figure 6). Fe^{3+} ions were consumed accompanied by O_2 evolution over Ag(I)-milled-$Na_2W_4O_{13}$ until a certain amount of Fe^{2+} ions were accumulated in the reactant solution. After 29 h of irradiation time, H_2 and O_2 evolved in a stoichiometric amount under visible light irradiation (second run in Figure 6). Water splitting proceeded even in the absence of $Fe^{3+/2+}$ of a redox couple accompanied by interparticle electron transfer as shown in Figure 7, as previously reported.[25,40] The activity was lower than that in the presence of $Fe^{3+/2+}$. No water splitting proceeded employing either Ru/$SrTiO_3$/Rh or Ag(I)-milled-$Na_2W_4O_{13}$ alone under visible light irradiation, indicating that both photocatalysts were necessary for the water splitting. Thus, the Ag(I)-milled-$Na_2W_4O_{13}$ has arisen as a new and useful O_2-evolving photocatalyst in Z-scheme systems for water splitting under visible light irradiation.

4. CONCLUSIONS

Parts of K^+ ions in $K_4Nb_6O_{17}$ and Na^+ ions in $Na_2W_4O_{13}$ were substituted with Ag^+ ions keeping the layered structures using a molten $AgNO_3$ treatment (Ag(I)-$K_4Nb_6O_{17}$ and Ag(I)-

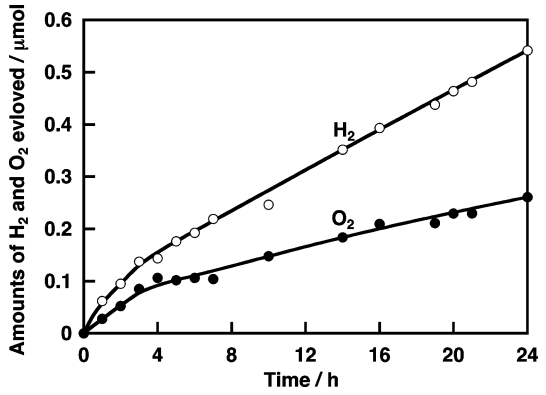

Figure 7. Z-Schematic water splitting into H_2 and O_2 using (Ru/$SrTiO_3$/Rh)-(Ag(I)-milled-$Na_2W_4O_{13}$) without electron mediator under visible light irradiation. Catalyst: 0.1 g of Ru/$SrTiO_3$/Rh and 0.2 g of Ag(I)-milled-$Na_2W_4O_{13}$, solution: 120 mL of an aqueous H_2SO_4 solution (pH3.5), light source: 300 W Xe-arc lamp with a long-pass filter (λ > 420 nm).

$Na_2W_4O_{13}$). The Ag(I)-$K_4Nb_6O_{17}$ and Ag(I)-$Na_2W_4O_{13}$ showed photocatalytic activities for O_2 evolution in the presence of sacrificial reagents utilizing the new absorption bands formed by the Ag(I)-substitution. The Ag(I)-$Na_2W_4O_{13}$ produced O_2 under visible light irradiation. When the $Na_2W_4O_{13}$ pulverized by ball milling was treated by a molten $AgNO_3$ (Ag(I)-milled-$Na_2W_4O_{13}$), the Ag(I)-substitution rate increased compared to Ag(I)-$Na_2W_4O_{13}$, giving the improved activity for O_2 evolution. Z-schematic water splitting under visible light irradiation was achieved by employing Ag(I)-milled-$Na_2W_4O_{13}$ of an O_2-evolving photocatalyst, Ru/$SrTiO_3$/Rh of a H_2-evolving photocatalyst. Thus, we successfully demonstrated that the Ag(I)-substitution by a molten $AgNO_3$ treatment was useful for development of visible-light-driven layered tungstate and niobate photocatalysts.

■ ASSOCIATED CONTENT

Supporting Information

SEM images and Diffuse reflectance spectra for $K_4Nb_6O_{17}$ and Ag(I)-$K_4Nb_6O_{17}$, SEM images, Lattice parameters, and Valence band region of XPS for $Na_2W_4O_{13}$, Ag(I)-$Na_2W_4O_{13}$, milled-$Na_2W_4O_{13}$, and Ag(I)-milled-$Na_2W_4O_{13}$. The Supporting Information is available free of charge on the ACS Publications website at DOI: 10.1021/acsami.5b01555.

■ AUTHOR INFORMATION

Corresponding Author

*E-mail: a-kudo@rs.kagu.tus.ac.jp (A.K.).

Notes

The authors declare no competing financial interest.

■ ACKNOWLEDGMENTS

This work was supported by a Grant in Aid (Nos. 24107001 and 24107004) for Science Research on Innovative Areas (Area no. 2406) from the Ministry of Education, Culture, Sports, Science and Technology (MEXT) in Japan. The authors gratefully thank Mr. K. Watanabe for assistance with data collection.

■ REFERENCES

(1) Kudo, A.; Miseki, Y. Heterogeneous Photocatalyst Materials for Water Splitting. *Chem. Soc. Rev.* **2009**, *38*, 253−278.

DOI: 10.1021/acsami.5b01555
ACS Appl. Mater. Interfaces 2015, 7, 14638−14643

(2) Osterloh, E. H. Inorganic Materials as Catalysts for Photochemical Splitting of Water. *Chem. Mater.* **2008**, *20*, 35−54.
(3) Kudo, A.; Tanaka, A.; Domen, K.; Maruya, K.; Aika, K.; Onishi, T. Photocatalytic Decomposition of Water over $NiO-K_4Nb_6O_{17}$ Catalysts. *J. Catal.* **1988**, *11*, 67−76.
(4) Kudo, A.; Kato, H. Photocatalytic Activities of $Na_2W_4O_{13}$ with Layered Structure. *Chem. Lett.* **1997**, *5*, 421−422.
(5) Maeda, K.; Tanaka, T.; Hara, M.; Saito, N.; Inoue, Y.; Kobayashi, H.; Domen, K. GaN:ZnO Solid Solution as a Photocatalyst for Visible-Light-Driven Overall Water Splitting. *J. Am. Chem. Soc.* **2005**, *127*, 8286−8287.
(6) Lee, Y.; Teramura, K.; Hara, M.; Domen, K. Modification of $(Zn_{1+x}Ge)-(N_2O_x)$ Solid Solution as a Visible Light Driven Photocatalyst for Overall Water Splitting. *Chem. Mater.* **2007**, *19*, 2120−2127.
(7) Asai, R.; Nemoto, H.; Jia, Q.; Saito, K.; Iwase, A.; Kudo, A. A Visible Light Responsive Rhodium and Antimony-Codoped $SrTiO_3$ Powdered Photocatalyst Loaded with an IrO_2 Cocatalyst for Solar Water Splitting. *Chem. Commun.* **2014**, *50*, 2543−2546.
(8) Maeda, K.; Lu, D.; Domen, K. Direct Water Splitting into Hydrogen and Oxygen under Visible Light by using Modified TaON Photocatalysts with d^0 Electronic Configuration. *Chem.—Eur. J.* **2013**, *19*, 4986−4991.
(9) Pan, C.; Takata, T.; Nakabayashi, M.; Matsumoto, T.; Shibata, N.; Ikuhara, Y.; Domen, K. A Complex Perovskite-Type Oxynitride: The First Photocatalyst for Water Splitting Operable at up to 600 nm. *Angew. Chem., Int. Ed.* **2015**, *54*, 2955−2959.
(10) Darwent, J. R.; Mills, A. Photooxidation of Water Sensitized by Tungsten Trioxide Powder. *J. Chem. Soc., Faraday Trans. 2* **1982**, *78*, 359−367.
(11) Kudo, A.; Omori, K.; Kato, H. A Novel Aqueous Process for Preparation of Crystal Form-Controlled and Highly Crystalline $BiVO_4$ Powder from Layered Vanadates at Room Temperature and Its Photocatalytic and Photophysical Properties. *J. Am. Chem. Soc.* **1999**, *121*, 11459−11467.
(12) Kato, H.; Kudo, A. Visible-Light Response and Photocatalytic Activities of TiO_2 and $SrTiO_3$ Photocatalysts Co-doped with Antimony and Chromium. *J. Phys. Chem. B* **2002**, *106*, 5029−5034.
(13) Kato, H.; Kobayashi, H.; Kudo, A. Role of Ag^+ in the Band Structures and Photocatalytic Properties of $AgMO_3$ (M: Ta and Nb) with the Perovskite Structure. *J. Phys. Chem. B* **2002**, *106*, 12441−12447.
(14) Ishii, T.; Kato, H.; Kudo, A. H_2 Evolution from an Aqueous Methanol Solution on $SrTiO_3$ Photocatalysts Codoped with Chromium and Tantalum Ions under Visible Light Irradiation. *J. Photochem. Photobiol., A* **2004**, *163*, 181−186.
(15) Konta, R.; Ishii, T.; Kato, H.; Kudo, A. Photocatalytic Activities of Noble Metal Ion Doped $SrTiO_3$ under Visible Light Irradiation. *J. Phys. Chem. B* **2004**, *108*, 8992−8995.
(16) Hosogi, Y.; Shimodaira, Y.; Kato, H.; Kobayashi, H.; Kudo, A. Role of Sn^{2+} in the Band Structure of SnM_2O_6 and $Sn_2M_2O_7$ (M = Nb and Ta) and Their Photocatalytic Properties. *Chem. Mater.* **2008**, *20*, 1299−1307.
(17) Ishikawa, A.; Takata, T.; Kondo, N. J.; Hara, M.; Kobayashi, H.; Domen, K. Oxysulfide $Sm_2Ti_2S_2O_5$ as a Stable Photocatalyst for Water Oxidation and Reduction under Visible Light Irradiation ($\lambda \leq 650$ nm). *J. Am. Chem. Soc.* **2002**, *124*, 13547−13553.
(18) Maeda, K.; Domen, K. New Non-Oxide Photocatalysts Designed for Overall Water Splitting under Visible Light. *J. Phys. Chem. C* **2007**, *111*, 7851−7861.
(19) Sayama, K.; Mukasa, K.; Abe, R.; Abe, Y.; Arakawa, H. Stoichiometric Water Splitting into H_2 and O_2 Using a Mixture of Two Different Photocatalysts and an IO_3^-/I^- Shuttle Redox Mediator under Visible Light Irradiation. *Chem. Commun.* **2001**, 2416−2417.
(20) Kato, H.; Hori, M.; Konta, R.; Shimodaira, Y.; Kudo, A. Construction of Z-Scheme Type Heterogeneous Photocatalysis Systems for Water Splitting into H_2 and O_2 under Visible Light Irradiation. *Chem. Lett.* **2004**, *33*, 1348−1349.
(21) Abe, R.; Takata, T.; Sugihara, H.; Domen, K. Photocatalytic Overall Water Splitting under Visible Light by TaON and WO_3 with an IO_3^-/I^- Shuttle Redox Mediator. *Chem. Commun.* **2005**, 3829−3831.
(22) Higashi, M.; Abe, R.; Ishikawa, A.; Takata, T.; Ohtani, B.; Domen, K. Z-Scheme Overall Water Splitting on Modified-TaON Photocatalysts under Visible Light ($\lambda < 500$ nm). *Chem. Lett.* **2008**, *37*, 138−139.
(23) Sasaki, Y.; Kato, H.; Kudo, A. $[Co(bpy)_3]^{3+/2+}$ and $[Co(phen)_3]^{3+/2+}$ Electron Mediators for Overall Water Splitting under Sunlight Irradiation using Z-Scheme Photocatalyst System. *J. Am. Chem. Soc.* **2013**, *135*, 5441−5449.
(24) Kudo, A. Z-Scheme Photocatalyst Systems for Water Splitting under Visible Light Irradiation. *Mater. Res. Bull.* **2011**, *36*, 32−38.
(25) Maeda, K. Z-Scheme Water Splitting Using Two Different Semiconductor Photocatalysts. *ACS Catal.* **2013**, *3*, 1486−1503.
(26) Sahoo, P. P.; Maggard, P. A. Crystal Chemistry, Band Engineering, and Photocatalytic Activity of the $LiNb_3O_8-CuNb_3O_8$ Solid Solution. *Inorg. Chem.* **2013**, *52*, 4443−4450.
(27) Kato, H.; Takeda, A.; Kobayashi, M.; Hara, M.; Kakihana, M. Photocatalytic Activities of $Cu_{3x}La_{1-x}Ta_7O_{19}$ Solid Solutions for H_2 Evolution under Visible Light Irradiation. *Catal. Sci. Technol.* **2013**, *3*, 3147−3145.
(28) Iwashina, K.; Iwase, A.; Kudo, A. Sensitization of Wide Band Gap Photocatalysts to Visible Light by Molten CuCl Treatment. *Chem. Sci.* **2015**, *6*, 687−692.
(29) Kato, H.; Fujisawa, T.; Kobayashi, M.; Kakihana, M. Discovery of Novel Delafossite-Type Compounds Composed of Copper(I) Lithium Titanium with Photocatalytic Activity for H_2 Evolution under Visible Light. DOI: 10.1246/cl.150341.
(30) Saito, N.; Kadowaki, H.; Kobayashi, H.; Nishiyama, H.; Inoue, Y. A New Photocatalyst of RuO_2-Loaded $PbWO_4$ for Overall Splitting of Water. *Chem. Lett.* **2004**, *33*, 1452−1453.
(31) Shimodaira, Y.; Kato, H.; Kobayashi, H.; Kudo, A. Investigations of Electronic Structures and Photocatalytic Activities under Visible Light Irradiation of Lead Molybdate Replaced with Chromium(VI). *Bull. Chem. Soc. Jpn.* **2007**, *80*, 885−893.
(32) Hosogi, Y.; Kato, H.; Kudo, A. Photocatalytic Activities of Layered Titanates and Niobates Ion-Exchanged with Sn^{2+} under Visible Light Irradiation. *J. Phys. Chem. C* **2008**, *112*, 17678−17682.
(33) Hosogi, Y.; Kato, H.; Kudo, A. Visible Light Response of $AgLi_{1/3}M_{2/3}O_2$ (M = Ti and Sn) Synthesized from Layered Li_2MO_3 using Molten $AgNO_3$. *J. Mater. Chem.* **2008**, *18*, 647−653.
(34) Sato, M.; Watanabe, J.; Uematsu, K. Crystal Structure and Ionic Conductivity of a Layered Perovskite, $AgLaNb_2O_7$. *J. Solid State Chem.* **1993**, *107*, 460−470.
(35) Toda, K.; Watanabe, J.; Sato, M. Synthesis and Ionic Conductivity of New Layered Perovskite Compound, $Ag_2La_2Ti_3O_{10}$. *Solid State Ionics* **1996**, *90*, 15−19.
(36) Shannon, R. D. Revised Effective Ionic Radii and Systematic Studies of Interatomic Distances in Halides and Chalcogenides. *Acta Crystallogr.* **1976**, *A32*, 751−767.
(37) Kinomura, N.; Kumada, N.; Muto, F. Ion Exchange of $K_4Nb_6O_{17}\cdot 3H_2O$. *J. Chem. Soc., Dalton Trans.* **1985**, 2349−2351.
(38) Pérez Flores, J. C.; Kuhn, A.; García Alvarado, F. Synthesis, Structure, and Electrochemical Li Insertion Behaviour of $Li_2Ti_6O_{13}$ with the $Na_2Ti_6O_{13}$ Tunnel-Structure. *J. Power Sources* **2011**, *196*, 1378−1385.
(39) Kinomura, N.; Kumada, N.; Muto, F. Ion Exchange of $K_4Nb_6O_{17}\cdot 3H_2O$. *J. Chem. Soc., Dalton Trans.* **1985**, *11*, 2349−2351.
(40) Sasaki, Y.; Nemoto, H.; Saito, K.; Kudo, A. Solar Water Splitting Using Powdered Photocatalysts Driven by Z-Schematic Interparticle Electron Transfer without an Electron Mediator. *J. Phys. Chem. C* **2009**, *113*, 17536−17542.

DOI: 10.1021/acsami.5b01555
ACS Appl. Mater. Interfaces 2015, 7, 14638−14643